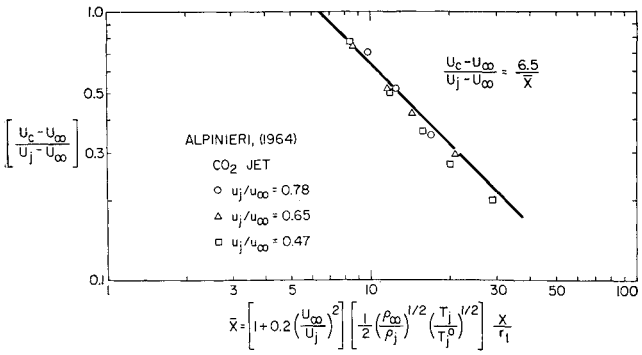

Fig. 3 Co-axial jet centerline velocity decay.

caused a decrease in the rate of spread of the central jet and the rate of growth of the half radius was no longer linear, furthermore, it was found that

$$(U_C - U_\infty)/(U_i - U_\infty) \propto 1/x$$

This result indicates that there is a possibility to define the proportionality constant such that the flow will be self-preserving. Applying the transformations reported for the stagnant external conditions did not yield the necessary transformation. It is necessary, also, to postulate that further transformation is possible, and that the proportionality constant is a function of the external fluid velocity such that $\beta = 1$ when $U_\infty = 0$. By analyzing the data reported in Ref. 9 we obtain $\beta = 1 + 0.2(U_\infty/U_i)^2$. Combining this result with Boynton's correlation we obtain an empirical result with good approximation.

$$(U_C - U_\infty)/(U_i - U_\infty) = 2(\rho_\infty/\rho_i)^{-1/2}\beta^{-1}\sigma r_i/x$$

Figure 3 shows the centerline velocity vs the normalized coordinate.

Conclusion

The results of this study imply that the Howarth transformation may be employed to reduce all fully developed jet velocity data to a common scale if a spreading constant that is a function of the Mach number is employed. Furthermore, applying a second spreading constant which is a function of the external flow condition it is possible to reduce data obtained in all coaxially flowing jets to a common scale. The significance of this finding cannot be assessed without more data.

References

[1] Townsend, A., *The Structure of Shear Flow*, Cambridge University Press, Cambridge, Mass., 1956, pp. 182–186.

[2] Kleinstein, G., "On the Mixing of Laminar and Turbulent Axially Symmetric Compressible Flows," Rept. 756, Feb. 1963, Polytechnic Institute of Brooklyn, Brooklyn, New York.

[3] Donaldson, C. and Gray, K. E., "Theoretical and Experimental Investigation of the Compressible Free Mixing of Two Dissimilar Gases," *AIAA Journal*, Vol. 4, No. 11, Nov. 1966, pp. 2017–2025.

[4] Howarth, P. L., "Concerning the Effect of Compressibility on Laminar Boundary Layers and Their Separation," *Proceedings of the Royal Society, London*, Vol. 194, 1948, pp. 16–42.

[5] Boynton, F., "Self-Preservation in Fully Expanded Round Turbulent Jets," *AIAA Journal*, Vol. 1, No. 9, Sept. 1963, pp. 2176–2178.

[6] O'Connor, T. J. et al, "Turbulent Mixing of an Axisymmetric Jet of Partially Dissociated Nitrogen with Ambient Air," *AIAA Journal*, Vol. 4, No. 11, Nov. 1966, pp. 2026–2032.

[7] Pai, S., *Fluid Dynamics of Jets*, D. Van Nostrand, New York, 1954, pp. 120.

[8] Smoot, L. D. and Purcell, W. E., "Model for Mixing of a Compressible Free Jet with a Moving Environment," *AIAA Journal*, Vol. 5, No. 11, Nov. 1967, pp. 2049–2052.

[9] Alpinieri, L., "An Experimental Investigation of the Turbulent Mixing on Nonhomogeneous Coaxial Jets," *AIAA Journal*, Vol. 2, No. 9, Sept. 1964, pp. 1560–1567.

Comments on the Convergence of Finite Element Solutions

KENNETH H. MURRAY*
Old Dominion University, Norfolk, Va.

I. Introduction

WITHIN the last few years, many developments have been made in the basic finite element. New trends toward curved elements to analyze curved structures have forced the profession to look closer at some basic concepts of the displacement function assumed for the element. This note deals with rigid-body mode shapes in displacement functions and their effect on the rate of convergence. Also considered is the effect of two shell theories and two load lumping procedures.

Some researchers[1,2] have included rigid-body mode shapes in their displacement functions for curved elements, but others[3] still insist they are not needed. There are researchers who do not include the rigid-body mode shapes, but correct the final displacement function or stiffness matrix, using equilibrium considerations.[4]

Cantin and Clough[2] point out that, for flat elements, the polynomial is the best displacement function assumption; but when a curved element is used, these polynomials cannot account for rigid-body motion. Therefore, if a structure, which has substantial rigid-body motion, is analyzed with these elements, convergence to a satisfactory solution is not always assured.

Walz, Fulton, Cyrus, and Eppink[5] show analytically that there is a large error term present in the curved element with the polynomial displacement function which does not have the provisions for unstrained rigid-body motion. They advance the idea that this large error could be due to the omission of the rigid-body mode shape. Of course, if when the mesh size is reduced, the rigid-body modes are recovered, slow convergence to a satisfactory result is possible. For this fine a mesh the flat element is equally as good.

The objective of this Note is to examine in greater detail the convergence for four different finite elements when used to analyze the circular arch presented in Ref. 5.

II. Elements

The standard straight and several curved elements were compared with each other with respect to their convergence to a satisfactory solution to the displacement of the example structure.

A. Straight element

The straight element stiffness matrix was derived using the following displacement function:

$$u = a_1 + a_2x \tag{1}$$

$$w = a_3 + a_4x + a_5x^2 + a_6x^3 \tag{2}$$

where u and w are the x and y displacements and the a's are generalized coordinates. This displacement function includes rigid-body mode shapes for the flat element structure and converges to an exact solution as shown in Ref. 5.

B. Curved elements

In all the curved elements, the displacement function has the following form:

$$u = f(s) \tag{3}$$

Received October 6, 1969; revision received November 3, 1969. This paper is the result of research conducted on the NASA-ASEE Summer Faculty Research Fellowship Program at Langley Research Center, Hampton, Va. The author extends a special thanks to R. E. Fulton for his help and guidance.

* Assistant Professor of Engineering.

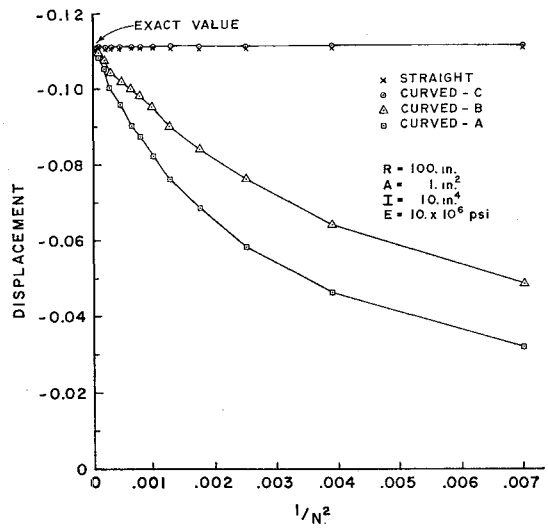

Fig. 1 Comparison of elements (date set 1).

$$w = g(s) \tag{4}$$

$$\theta = \frac{\partial w}{\partial s} + \frac{u}{R} \tag{5}$$

$$\epsilon_1 = \frac{\partial u}{\partial s} - \frac{w}{R} - y\left[\frac{\partial w^2}{\partial s^2} + \frac{1}{R}\frac{\partial u}{\partial s}\right] \tag{6}$$

$$\epsilon_2 = \frac{\partial u}{\partial s} - \frac{w}{R} - y\left[\frac{\partial w^2}{\partial s^2} + \frac{w}{R^2}\right] \tag{7}$$

where u = tangential displacement, w = radial displacement, θ = rotation in the $u - w$ plane, ϵ_1 = strain using the Timoshenko shell theory, ϵ_2 = strain using the Flügge shell theory, s = length along element, R = radius of curved element, and y = distance from centroidal surface of cross section of the arch. In each case, the displacement function satisfies the constant strain condition and is continuous over the length.

Each element was derived using the Timoshenko shell theory and the Flügge shell theory. These differ only in the curvature term, with Timoshenko using $(1/R)\partial u/\partial s$ and Flügge using w/R^2 [Eqs. (6) and (7)]. Each element was also derived using two different load lumping procedures. The first was a simple system where the load is calculated by multiplying the load value at the node by half the distance between adjacent nodes to each side. The second procedure, usually referred to as consistent load lumping, defines an equivalent nodal load system by equating external work of the original and equivalent systems.

1. Curved element with polynomial displacement function: A curved element stiffness matrix was derived using the displacement function defined by Eqs. (1) and (2), except x is replaced by s, the arc length. This displacement function does not allow unstrained rigid-body motion.

2. Transformed element: A curved element with the same displacement function as the straight element, except x is now the projected s length along the x axis, was transformed into arch coordinates using only trigonometric relations. This displacement function has rigid-body modes in the projection plane and, therefore, when transformed should still allow unstrained rigid-body motion.

3. Cantin and Clough curved element: Cantin and Clough[2] present a curved shell element which was reduced to an arch element with the following results:

$$u = a_1 s - a_2 R(1 - \cos\phi \cos\beta) + a_3 \cos\phi - a_4 \sin\phi \tag{8}$$

Table 1 Properties of the example arch

Property	Set 1	Set 2	Set 3
Total angle of arch	$\pi/4$	$\pi/4$	$\pi/4$
Cross-sectional area	1.0 in.^{2}	4.0	10.0
Cross-sectional moment of inertia	10.0 in.^{4}	1.33	1.0
Radius of centroidal axis	100.0 in.	100.0	20.0
Modulus of elasticity	10×10^6 psi	10×10^6	10×10^6

$$w = a_5 s^3 + a_6 s^2 - a_3 \sin\phi - a_4 \cos\phi - a_2 R \sin\phi \cos\beta \tag{9}$$

where ϕ is the angle measured clockwise from the bisector radius and β is half the total angle of the arch.

III. Results

Each element was used to analyze the example circular arch of Ref. 5. The properties of the example arch are given in Table 1. This arch behaves in an inextensional manner with some rigid-body motion. It was chosen as an example because it points up a basic problem in the curved element with the polynomial displacement function, as shown in Ref. 5.

In order to compare the convergence rates of the four elements, the number of elements per arch was varied from 8 to 80. The loading system is sinusoidal with one positive wave on the left half of the arch and a negative wave on the right half.

Figure 1 shows graphically the relative convergence of each of the elements with the first set of data which is representative of all sets.

Although not shown explicitly here, the two shell theories had no effect on the finite element convergence rate with respect to the example problem. Likewise, the two lumping procedures had no effect on the results for each element and data set.

IV. Conclusions

The exclusion of rigid-body modes from the displacement function reduces the convergence rate. The straight element, which allows unstrained rigid-body motion, is much better than a curved element which does not take into account rigid-body motion in analyzing a circular arch. As can be expected, the curved element that allows unstrained rigid-body motion (Cantin and Clough element) is better than the other three elements.

The Timoshenko and Flügge strain theories have no effect on the finite element convergence rate with respect to the example problem. It was thought at one time that the accuracy of the finite element method could be dependent on which shell theory was used, but this does not appear to be the case. The same conclusion can be drawn concerning the two load lumping procedures.

References

[1] Jones, R. E. and Strome, D. R., "Direct Stiffness Method Analysis of Shells of Revolution Utilizing Curved Elements," *AIAA Journal*, Vol. 4, No. 9, Sept. 1966, pp. 1519–1525.

[2] Cantin, G. and Clough, R. W., "A Curved, Cylindrical-Shell, Finite Element," *AIAA Journal*, Vol. 6, No. 6, June 1968, pp. 1057–1062.

[3] Haisler, W. E. and Stricklin, J. A., "Rigid-Body Displacements of Curved Elements in the Analysis of Shells by the Matrix-Displacement Method," *AIAA Journal*, Vol. 5, No. 8, Aug. 1967, pp. 1525–1527.

[4] Utku, S., "Stiffness Matrices for Thin Triangular Elements of Nonzero Gaussian Curvature," *AIAA Journal*, Vol. 5, No. 9, Sept. 1967, pp. 1959–1967.

[5] Walz, J. E. et al., "Accuracy of Finite Element Approximations to Structural Problems," TN D-5728, 1970, NASA.